Periodic density functional study of Rh and Pd interaction with the (1 0 0)MgO surface

T. Mineva [a], V. Alexiev [b], C. Lacaze-Dufaure [c], E. Sicilia [d], C. Mijoule [c], N. Russo [d,]

[a] UMR 5253 CNRS/ENSCM/UM2/UM1, Institut Charles Gerhardt Montpellier, 8 rue de 1' Ecole Normale, 34296 Montpellier Cedex 5, Fı
[b] Institute of Catalysis, BAS, G. Bonchev Str. 11, 1113 Sofia, Bulgaria
[c] CIRIMAT, Institut National Polytechnique de Toulouse, 118 route de Narbonne, 31077 Toulouse Cedex 4, France
[d] Dipartimento di Chimica, Universita' della Calabria, via P. Bucci, 87036 Arcavacata di Rende (CS), Italy

A B S T R A C T

The adsorption geometry and electronic properties of palladium and rhodium atoms deposited on the regular (1 0 0)MgO surface were analyzed by means of periodic DFT calculations using local, gradient-corrected and hybrid (B3LYP) functionals. Spin-polarized computations revealed doublet spin state of Rh atom to be the most stable electronic state for the adsorbed rhodium atom on (1 0 0)MgO. The preferred adsorption site of the metal (Pd and Rh) atoms was found to be the site on top of the surface oxygen atoms. A relatively stable geometry for the adsorption of the Pd and Rh in a bridge position above the two surface oxygens was found as well. The electronic structures suggested partly covalent bonding with contribution from electrostatic attraction between the metal and the oxygen atoms for both optimized structures. Small charge transfer was obtained from the support to the Pd and Rh metal atoms. The calculations showed that rhodium was bound stronger to the substrate probably due to stronger polarization effects.

Keywords:
Periodic density functional calculations
(1 0 0)MgO surface
Rhodium and palladium adsorption
Geometrical and electronic properties
Spin-polarized periodic calculations

1. Introduction

Interaction of transition metals with oxide surfaces retains the researchers' interest for several decades mainly due to its practical use in the field of heterogeneous catalysis [1,2]. The non-polar (1 0 0) surface of magnesium oxide is one of the most studied theoretically. Its relatively simple structure does not undergo significant relaxation or reconstruction and provides a good model for testing new theoretical approaches and describing adsorption features of small probe molecules or deposited transition metal (TM) atoms, clusters and layers.

Embedded cluster models have been extensively employed in the description of the electronic and geometrical structures of Pd atoms and dimers nucleated on regular or defect sites on the (1 0 0)MgO surface (see for example Ref. [3–7]). Adsorption of CO and C_2H_2 on supported Pd atoms was investigated using the same cluster structures to describe various surface defects [4,5]. The latter systems were studied as well by periodic slab computations [5–7]. The results obtained by both cluster and periodic techniques agreed in the prediction of the nucleation and dimerization of Pd atom(s) on the regular and defect centers. Other transition metal (TM) atoms, such as Ag, Rh and Au nucleated in different (1 0 0)MgO surface sites represented by the above cited clusters were also considered [8–10] with main purpose to bring complementary understanding to the experimental data about possible TM nucleation positions. These results favor adsorption of small molecules on the supported metals trapped on charged centers depending on the chemical nature of both the adsorbate [4,7] and the transition metal atom [8,10]. All these studies support the overall agreement that the catalytic processes at oxide surfaces proceed on various type of defects. Still a fundamental understanding of these observations is absent.

Fewer articles consider the long-range effect on the nucleation and properties of deposited metal atoms on MgO surfaces with imposed periodic boundary conditions [11–20]. It was established from the slab model calculations [14] that the steps, corners and reverse corner sites of the (1 0 0)MgO surface undergo significant relaxation in contrast to the regular surface. Furthermore, the relaxed geometries affect the electronic structures raising the F-center level energy close to the top of the valence band [14]. Studies based on first principles periodic approach [12,13] on the deposition of several 4d transition metals (including Pd) on the stochiometric MgO favor the metal adsorption on top of the surface oxygen atoms.

The Rh atom adsorption or layer deposition on the magnesium oxide surfaces have been less investigated by the periodic slab models. To our knowledge there are only few works comparing the geometries and electronic properties of Pd and Rh atoms on a (1 0 0)MgO slab [17,18,20]. The influence of various rhodium

Corresponding author.
E-mail address: nrusso@unical.it (N. Russo).

coverages on (1 0 0)MgO on the adhesion and adsorption energies was recently investigated using periodic plane-wave methods [19]. The open shell electronic configuration of the rhodium ground state, that is ^4F ($4d^8 5s^1$) requires spin-polarized computations, contrary to the electronic structure of the Pd atom with ground state ^1S ($4d^{10}ds^0$). Despite the fact that the total magnetic moment of Rh atom persist upon adsorption most of the periodic Rh/MgO results refer to the spin non-polarized computations. Consideration of the spin-polarization effect [20] using the gradient-corrected functional gave only 0.30 eV stabilization for the Rh/(1 0 0)MgO system.

In this work we focus on the geometrical and the electronic properties of Rh and Pd atoms on regular (1 0 0) surface of MgO as obtained from first principle periodic density functional computations. The performance of local density approximations (LDA), generalized gradient-corrected approximations (GGA) and the hybrid B3LYP functional is also examined taking into account spin-polarization effect for Rh/MgO system. Analysis of the band structures and the density of states for the Rh and for the Pd atoms on the magnesium oxide surface give details of the metal interaction with the substrate. We believe that such a comparison is of interest, as many recent experimental studies on the Pd/MgO model catalytic systems [21–28] address the question weather the palladium can be used as an alternative to the expensive rhodium in the reaction of reduction of NO by CO [29].

2. Computational details

The calculations were performed using Crystal98 [30] code. In this program the atomic orbitals are represented as linear combinations of Gaussian type functions. In this study, Mg/O atoms were described with 86-1G/8-511G all electron basis set [31], while for the Pd and Rh atoms the HAY&WADT-Large core [32] effective core potentials were employed.

Computations were carried out at the Density Functional (DF) level of theory using local density approximation (LDA), gradient-corrected approximation (GGA) and hybrid (B3LYP [33]) exchange-correlation functionals. The local spin-density approximations for the exchange and correlation functionals were the Dirac-Slater approximation [34] and the Perdew and Zunger parametrization [35] of the Ceperley-Alder correlation functional, respectively. The GGA is based on the algorithm of Perdew and Wang for the exchange [36] and correlation [37] potentials. Computational tolerances for controlling the accuracy of Coulomb and exchange and correlation series were set equal to: 10^{-5}, 10^{-5}, 10^{-5}, 10^{-5}, 10^{-11}.

To study the surface properties of (1 0 0)MgO, calculations were performed on a model slab that was infinitely periodic in two dimensions (x and y) and consisted of six atomic layers parallel to the exposed surface. The interaction of Pd and Rh atoms with the (1 0 0)MgO surface was investigated using a model represented by a (2×2) supercell (1/4 ML) in order to avoid the lateral interaction between the adsorbed metal atoms.

Geometrical optimizations of the lattice constant of bulk MgO, the surface Mg and O ionic positions and the nucleation positions of Rh and Pd atoms (on top of one O^{2-} and bridging two adjacent surface oxygen ions) were done numerically using repeated line search. In order to describe MgO surface buckling, the outermost Mg and O ions were allowed to move in z-direction. The x, y and z coordinates of Pd and Rh atoms were left unconstrained in the optimization procedure.

In the case of Rh/MgO system spin-polarized computations were performed additionally, assuming doublet and quartet spin states. The results presented throughout this work are those for the most stable doublet state.

3. Results and discussion

3.1. Geometrical parameters and electronic structure of bulk MgO and the regular (1 0 0)MgO surface

To examine the reliability of the models and functionals employed in this study we first optimized MgO lattice constant a_0. The results obtained were 4.154, 4.233 and 4.184 Å at the LDA, GGA and B3LYP levels of theory, respectively. Both GGA and B3LYP values match well the experimental lattice constant of $a_0 = 4.213$ Å [38]. Comparing our results for the MgO lattice constant, we note their reasonable agreement with previous data obtained with Crystal code using larger basis set [39]. Moreover, post-correlated Hartree–Fock (HF) computations [39] yielded values of 4.101 and 4.105 Å depending on the type of approximation for the correlation energy.

It is already documented [18,19,39,40] that the structural perturbation of the bulk terminated (1 0 0)MgO is small, associated with a small relaxation and a nonzero rumple at the (1 0 0) surface. The experimental and theoretical data for the relaxation and rumpling of (1 0 0)MgO surface available in the literature are scattered approximately 15% according to the differences in the experimental conditions and sample preparation [41,42], and the level of theoretical models [18,19,39,40]. Our results for the relaxation and rumpling fall in the range of the experimental [41,42] and previously computed values [18,19,39,40]. The largest amount of relative inward and outward displacements of the surface cations and anions, obtained in this work, are predicted from the GGA calculations: $\Delta z = -0.023$ Å (Mg^{2+}) and $\Delta z = 0.017$ Å (O^{2-}). B3LYP and LDA Δz values are respectively, -0.015 and -0.018 Å for the magnesium cation, and 0.007 and 0.011 Å for the oxygen anion.

Convergence of the surface energies E_s was tested for slabs consisting of up to nine layers. Increasing the number of layers from six to nine we found insignificant change in the E_s of about 8.10^{-3} eV/Cell. Therefore we choose six layers to represent the (1 0 0)MgO surface for the computations with the Pd and Rh adsorption. Comparing the surface energy values of 0.898 (LDA), 0.789 (GGA) and of 0.735 eV/cell (B3LYP) with the experimentally reported data [43] that varies between 0.571 and 0.653 eV/cell we find a general overestimation of about 0.3 eV/cell with LDA and of about 0.1 eV/cell with B3LYP methods. However the experimental incertitude is of about 15% and the B3LYP overestimation is of 20%, if the averaged experimental value is taken. The computed E_s values are similar to the previously obtained in the HF [39,40,44] and in the DFT (Perdew–Wang GGA functional) [45] studies, where the reported DFT surface energies are computed per unit surface area and not per cell. For a straightforward comparison with those DFT results we report the surface area values obtained by us: 8.86, 8.93 and 8.75 A^2 for the LDA, GGA and B3LYP functionals, respectively.

Analysis of the bulk MgO band structure and surface states of the 6-layers slab of (1 0 0)MgO are similar to previous studies for 3- and 5-layers slabs [40,44,46].

3.2. Adsorption geometries of Pd/(1 0 0)MgO and Rh/(1 0 0)MgO

We found two possible nucleation sites for Pd and Rh on the (1 0 0)MgO surface using a [2×2] supercell model. Both adsorbate structures are shown in Fig. 1a and b. The site on top of the O^{2-} ions of the surface (Fig. 1a) has been already distinguished from the previous theoretical studies [17,18,20] as the most favorable adsorption position for the Pd atom. Our results yielded an energetically stable structure also for the TM atoms in a position bridging two surface oxygen anions (Fig. 1b). Although, the TM atoms were allowed to move in the three directions over the surface (vide supra) no stable adsorption configuration was located on top of the

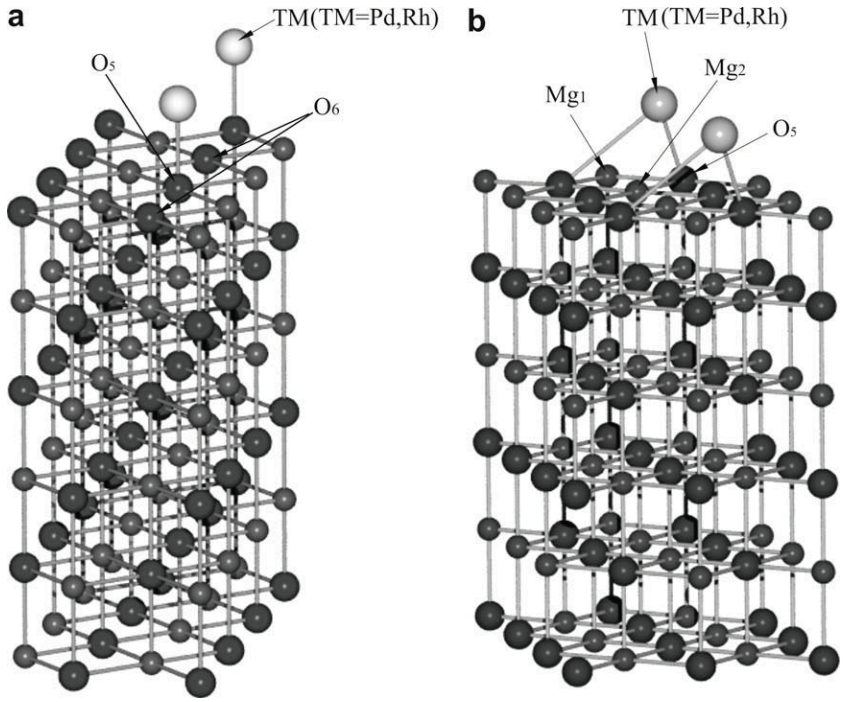

Fig. 1. Slab models used to study Pd and Rh atoms adsorped (a) on top of one oxygen atom and (b) in bridge position between two oxygen atoms.

Table 1
Important geometrical parameters of adsorbed TM (Pd, Rh) atoms on top of O^{2-} anions. For the atomic numbers see Fig. 1. Distances R are in Å and angles α in degree.

Method	$R_{\text{Pd-surf}}$	α (Pd-O5-Mg1)	$R_{\text{Rh-surf}}$	α (Rh-O5-Mg1)
LDA	1.982	90.0	2.251	90.9
GGA	2.250	91.6	2.494	91.1
B3LYP	2.084	91.1	2.135	91.2

Mg^{2+} ion. The latter findings agree with the already reported results by several authors that Pd [17,18,20] and Rh [17,19,20] atoms do not adsorb or adsorb very weekly on top of the magnesium cations.

The optimized geometrical parameters for the Pd and the Rh atoms nucleated on top of O^{2-} and bridging two O^{2-} ions are given in Tables 1 and 2, respectively. In the case of metal adsorption on top of surface oxygen (Table 1), the three type of functionals yielded similar distances between the TM atoms and MgO (100) surface ($R_{\text{TM-surf}}$). Rh atom optimal position is found to be further removed from the surface than that of Pd. However, at B3LYP level of theory the Pd and Rh distances to the surface differ only by 0.05 Å. Our GGA and B3LYP $R_{\text{Rh-surf}}$ values are slightly higher than those cited in Ref. [19], where $R_{\text{Rh-surf}}$ is 1.99 Å for 1/8 ML coverage. In general, a good agreement is established between the geometrical parameters obtained in this work and the reported theoretical values for Rh/(100)MgO surface (2.09 Å [17] and 2.01 Å [20]) and for Pd/(100)MgO (2.06 Å [17]) at low-coverage.

For the bridge adsorption site, the adsorption geometry depends on the functional used. At the B3LYP level of theory we found that the optimized bridging position of the metal atom is not symmetrical relatively to the substrate oxygen atoms from the first layer. The TM atom is shifted towards one of the oxygen atoms. Hence, the bond lengths between the Pd (Rh) atom and surface oxygen anion were obtained to be shorter compared to the results computed with LDA and GGA approximations.

Again the $R_{\text{Rh-surf}}$ is larger than the distance between Pd and the substrate. At lower coverage the Rh-surface distance reported in Ref. [19] for bridge Rh adsorption is slightly shorter ($R_{\text{Rh-surf}}$ = 1.80 Å [19]) than our values. We note the overall agreement between the theoretical data and the experimentally established Rh—O bond length of 1.95 Å using Extended X-ray adsorption fine structure spectroscopy (EXAFS) for highly dispersed Rh particles [47]. To our knowledge, bridge adsorption position was not reported for Pd atom on MgO regular surfaces.

3.3. Adsorption energies of Pd/(100)MgO and Rh/(100)MgO: effect of spin-polarization for the Rh/MgO system

The adsorption energies (E_a) and the Mulliken atomic net charges computed for both Pd and Rh/(100)MgO structures are collected in Table 3. The adsorption energies were computed as difference between the sum of energies of the isolated transition metal atom (E_{TM}) and the (100)MgO buckled surface($E_{(100)\text{MgO}}$), and the energy of the TM/(100)MgO system ($E_{\text{TM/(100)MgO}}$): $E_a = [E_{(100)\text{MgO}} + E_{\text{TM}}] - E_{\text{TM/(100)MgO}}$.

An important issue for the accurate computations of the DF adsorption energies in the studied cases is the way the ground state energies of the Rh and Pd atoms are calculated. Whereas Pd atom has fully occupied 4d shell that does not give rise to nearly degenerate

Table 2
Important geometrical parameters of adsorbed TM (Pd, Rh) atoms in bridge position between two O anions. For the atomic numbers see Fig. 1. Distances R are in Å.

Method	$R_{\text{Pd-surf}}$	$R_{\text{Pd-O5}}$	$R_{\text{Pd-O6}}$	$R_{\text{Pd-Mg1}}$	$R_{\text{Rh-surf}}$	$R_{\text{Rh-O5}}$	$R_{\text{Rh-O5}}$	$R_{\text{Rh-Mg1}}$
LDA	1.877	2.426	2.427	2.445	2.082	2.548	2.544	2.567
GGA	2.029	2.674	2.674	2.112	2.038	2.609	2.607	2.998
B3LYP	2.081	2.155	3.529	2.724	2.106	2.145	3.307	2.792

Table 3
Adsorption energies (E_a) in eV and Mulliken charges q for Rh and Pd adsorbed (a) on top of O anion and (b) in bridge position between two O anions.

Method	Pd/(100)MgO				Rh/(100)MgO			
	^aE_a	^bE_a	^aq	^bq	^aE_a	^bE_a	^aq	^bq
LDA	2.56	2.22	−0.35	−0.31	2.88	2.73	−0.33	−0.41
GGA	1.77	1.59	−0.25	−0.22	1.92	1.75	−0.27	−0.39
B3LYP	1.36	1.35	−0.22	−0.25	1.59	1.53	−0.27	−0.30

low lying energy terms, the Rh atomic ground state $^4F(4d^8s^1)$ is only 0.34 eV lower than the first excited ^2D (d^9) state and often the DF electronic structure computations predict the ^2D state to be the most stable one. So, the first difficulty arises with the description of the lowest electronic state of the isolated atom. For this reason, the Rh adsorption energies (Table 3) were calculated by imposing spin-polarization for the quartet spin state of the isolated Rh atom. The spin-polarized calculations correctly predict quartet Rh atom to be more stable than the doublet. Therefore E_{TM} value used for adsorption energy calculations is the energy value of Rh atom in its quartet ground state as computed by us from the spin-polarized DFT.

In addition, it is not a trivial task to conclude a priory which one of the ^4F and ^2D states of Rh determines the ground state energy of the unit cell of the (100)MgO surface with the adsorbed Rh atom. In order to examine the effect of the net magnetic moment of Rh atom upon adsorption, we performed computations for the fully spin-polarized Rh/(100)MgO structures assuming doublet and quartet spin states. The results indicate the spin-polarized structures with one unpaired electron as the most stable ones. The quartet state is less stable than the doublet one by 1.46 eV (B3LYP), 1.31 (GGA) and 1.15 eV (LDA) for Rh on top of one oxygen.

The difference between the spin non-polarized and spin-polarized approaches using LDA and GGA functionals is not large. The spin-polarized computations of the Rh on top of the surface oxygen give more stable energies by 0.18 eV (LDA) and 0.14 eV (GGA) and for Rh adsorption bridging two oxygen anions – by 0.08 eV (LDA) and 0.36 eV (GGA). The results concerning the spin-polarization effects obtained in this work at the GGA level are close to those reported in Ref. [20] (0.36 eV in Ref. [20]). The hybrid B3LYP functional predicts much stronger effect of the spin-polarization. Indeed, the B3LYP computations with accounting explicitly for the spin-polarization led to energy stabilizations by 0.83 eV (on top configuration) and by 0.87 eV (bridging rhodium position).

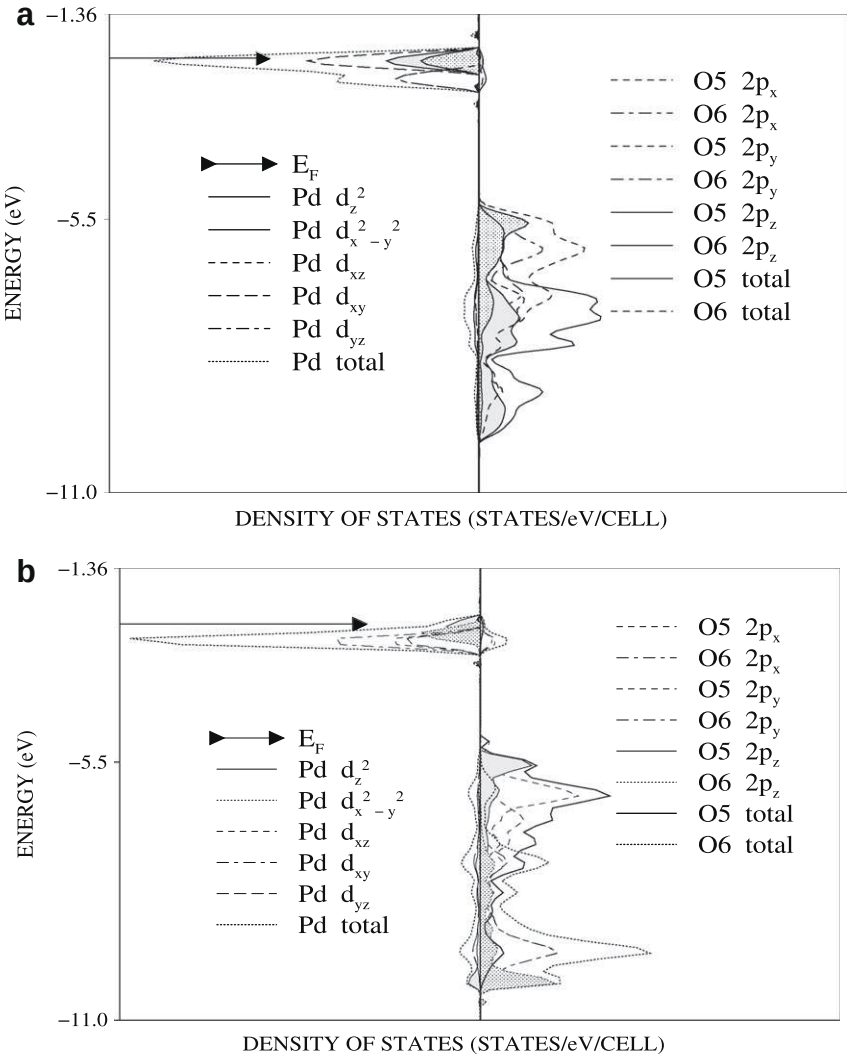

Fig. 2. Projected DOSS of Pd 4d (left) and O 2p (right) orbitals from the surface layer of MgO for Pd atom (a) on top of the O^{2-} and (b) bridging two surface oxygen ions obtained with B3LYP exchange-correlation functional. Atomic numbers are given in Fig. 1.

As seen from the E_a values in Table 3, the LDA functional predicts stronger TM-substrate bonding compared to the values obtained with the GGA and the hybrid methods. The adsorption energies computed with the three different approximations for the exchange-correlation density are spread within 1.5 eV for the on top and within 0.7 eV for the bridge structures. The results favored the on top site and reveal stronger Rh bonding to the substrate. Previously calculated low-coverage E_a values [17,18,20] suggested similar trend.

At B3LYP level the on top position is favoured by 0.06 eV in case of Rh coverage and by only 0.01 eV in the case of Pd adsorption. The latter results are however expected since the B3LYP method yielded similar values for the TM–O distances in the cases of bridge and on top adsorption (see Table 2), e.g. the TM atom in the bridge adsorption site is shifted towards one of the oxygen atoms.

Adsorption energy for Pd on MgO(001) of 1.2 eV is deduced from analysis of Pd growth on magnesium oxide (001) surface with variable-temperature atomic force microscopy [48] and our B3LYP E_a values agree well with this experimental result.

The amount of the net metal charges as obtained from the Mulliken population analysis, given in Table 3 show a small electron transfer from the surface anions to the metal atoms. This process is obviously accompanied with the reduction of the net atomic charges of the surface O ions bound to the metal atom.

3.4. Electronic structures of Pd/(100)MgO and Rh/(100)MgO systems: effect of the adsorption site and of the exchange-correlation functional

In all the studied cases the modifications due to the TM adsorption of the electronic structure of the (100)MgO surface are constrained to the first layer of the magnesium oxide. The main changes consist of the appearance of the metal induced states in the band gap of the MgO surface, showing a little dispersion along Γ–X–W–Γ. Their position with respect of the MgO valence band is determined by the energy of metal states.

The projections of the density of states (DOS) on chosen sets of TM atomic 4d (left) and oxygen 2p (right) orbitals from the surface layer of (100)MgO at B3LYP level are displayed in Figs. 2 and 3 and those at LDA level are given in Figs. 4 and 5. The LDA, GGA and B3LYP functionals yielded a perturbed structure of the surface oxygen 2p band: (i) additional peaks emerge in the region of the metal PDOS and (ii) new bands due to the filled O $2p_z$ states appear at the lower end of the surface valence band at Γ. The overall position of

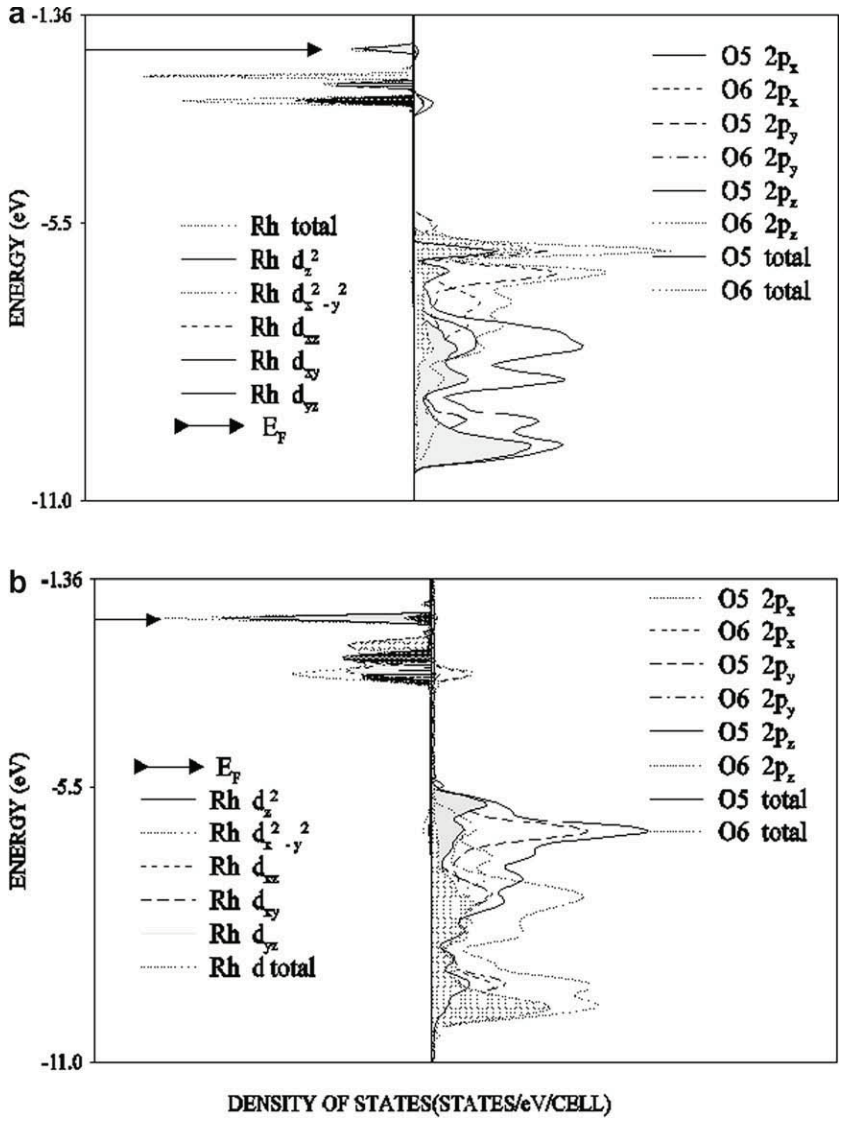

Fig. 3. Projected DOSS of Rh 4d (left) and O 2p (right) orbitals from the surface layer of MgO for Rh atom (a) on top of the O^{2-} and (b) bridging two surface oxygen ions obtained with B3LYP exchange-correlation functional. Atomic numbers are given in Fig. 1.

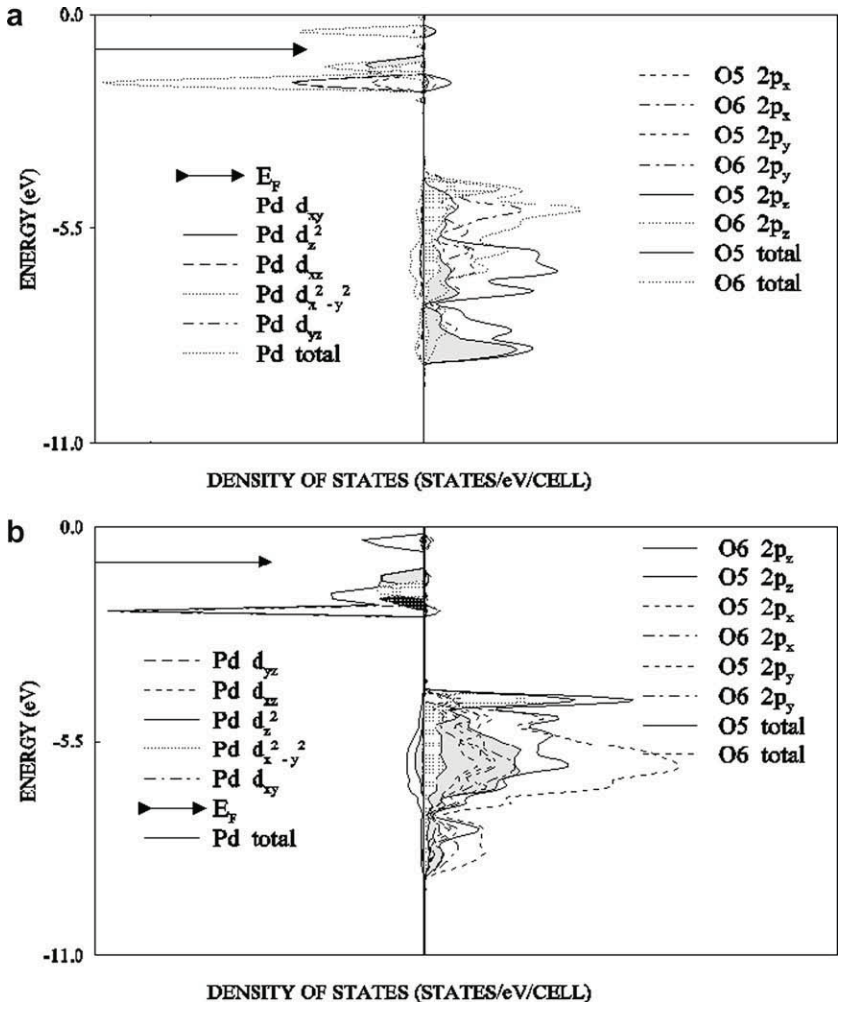

Fig. 4. Projected DOSS of Pd 4d (left) and O 2p (right) orbitals from the surface layer of MgO for Pd atom (a) on top of the O^{2-} and (b) bridging two surface oxygen ions obtained with LDA exchange-correlation functional. Atomic numbers are given in Fig. 1.

the first MgO layer valence band is shifted slightly towards lower energies with respect to the clean surface.

The adsorption of Pd(Rh) atoms on top of the oxygen of the substrate proceeds by formation of two type of bonds. One is between metal $4d_z^2$ orbitals and oxygen $2p_z$ orbitals. This type of bonding induces pronounced downward shift of O $2p_z$ band, while the metal $4d_z^2$ band is shifted upward. Significant part of the $4d_z^2$ states (antibonding) is above the Fermi level and overall contribution from these bonds to the adsorption energy is positive. For the other type, the bonding is between metal $4d_{xz}$ and $4d_{yz}$ orbitals and combinations of oxygen $2p_x$ and $2p_y$ orbitals. The respective bands composed by these orbitals are filled and positioned bellow the E_F thus the overall effect is repulsive For the optimized bridging position of the metal atom, the adsorption site is not symmetrical relative to the substrate oxygen atoms from the first layer. Therefore, the coupling between oxygen and metal d orbitals which enhances TM–O bonding involves different combinations of 2p orbitals from the surface oxygens. The set which contributes to the TM–O bonding consists of metal $4d_z^2$, $2p_z$ from the nearest O and $p_x(p_y)$ orbitals from the second oxygen. Significant number of states from this band is antibonding (e.g. above the Fermi level). Only this type of bonding contributes to the adsorption energy. The rest of the formed TM–O bonds do not contribute to the adsorption energy and involve a combinations of filled O $2p_x(p_y)$ and other metal 4d orbitals. These states are found bellow the Fermi level.

Our result show that for both considered metal adsorption sites the bonds formed between surface oxygens and the metal atoms are partly covalent and an additional stabilization of adsorbed metals on Mg(100) surface is due to the polarization. This is substantiated by the calculated small overlap population of TM–O bonds and by the electron transfer towards Pd (Rh) atoms from the first MgO layer (Table 3). The latter is probably the reason for the already mentioned downward shift of the 2p surface O valence bands with respect to the clean surface. Nevertheless, the band structures of Pd and Rh adsorbed on MgO show comparable characteristics, these systems exhibit different electronic properties. The rhodium covered MgO surfaces are found to be metallic for both studied adsorption sites and at the LDA/GGA/B3LYP levels of DF approximations, while the Pd/MgO systems are calculated as semiconducting with an optical gap of 2.6 eV for B3LYP and metallic for LDA and GGA DF approximations. The angular momentum decomposed DOS obtained from B3LYP calculations for Pd and Rh shown in Figs. 2a and b and 3a and b reveal larger separation between the bonding oxygen $2p_z$ and metal $4d_z^2$ states for Rh in both adsorption sites, indicating stronger bonding to the substrate.

Moreover the integrated density of antibonding states above the Fermi level for adsorbed Rh is higher, despite the lower number of electrons with respect to that of adsorbed Pd. The reason for this is probably due to the stronger interaction between Rh $4d_z^2$ and O $2p_z$ orbitals giving rise to an upward shift of the metal d states

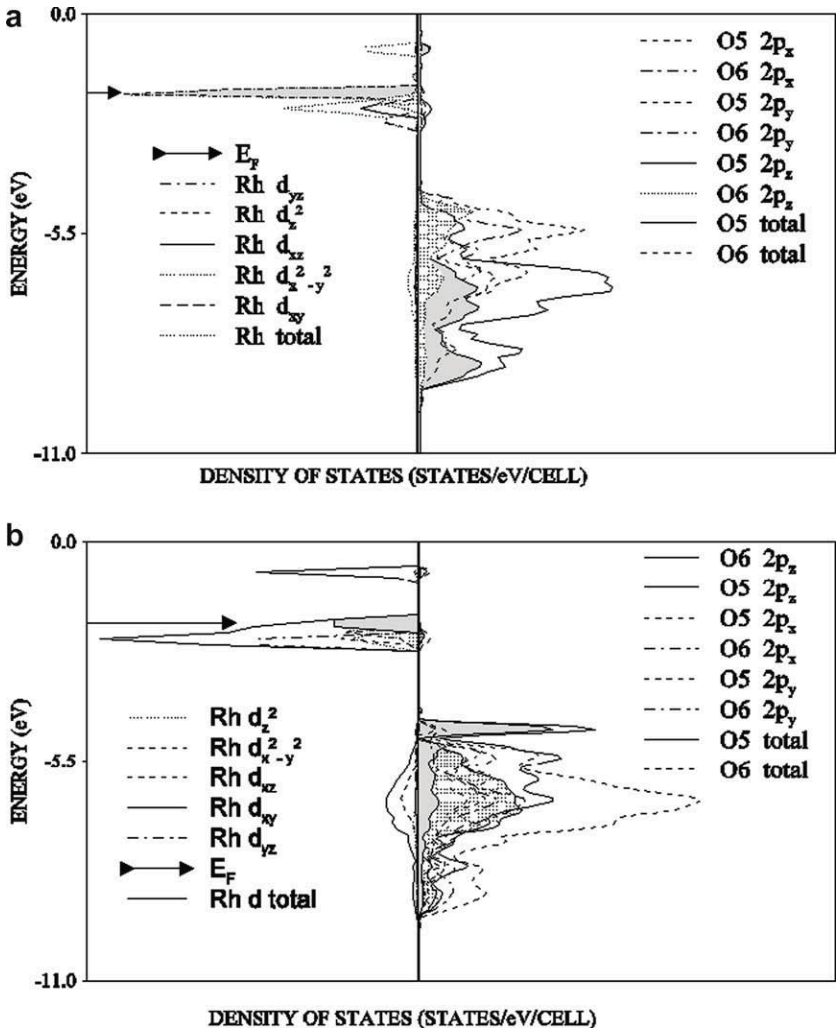

Fig. 5. Projected DOSS of Rh 4d (left) and O 2p (right) orbitals from the surface layer of MgO for Rh atom (a) on top of the O^{2-} and (b) bridging two surface oxygen ions obtained with LDA exchange-correlation functional. Atomic numbers are given in Fig. 1.

above Fermi level. We note also the broader spread of the Rh d states for both studied adsorption sites. The proposed model of metal–substrate bonding therefore agrees with the already reported bonding schemes for mono-layers of 4d transition metals on MgO by Goniakowski [13].

For the adsorption of metal atoms in a bridging position to two surface O ions the interaction is essentially with the nearest oxygen. However, the second oxygen is also involved in the bond formation and states from the bottom of the metal 4d valence and O $2p_x(p_y)$ bands participate in the bonding. For this type of adsorption of Rh obtained within B3LYP approximation we observe a diminished spacing between the closest oxygen $2p_z$ and metal $4d_z^2$ states. The antibonding and bonding states arising from the interaction with the second O are found bellow Fermi level and the spacing between these states is much smaller. For Pd adsorbed in a bridging sites the $2p_z$ band from the closest O is found at the bottom end of O 2p valence band with even smaller downward shift, thus the bonding between the surface and the deposit weakens. We note that for the B3LYP approximation the metal in its optimized bridging position sits nearly on top of the one of the oxygens from the MgO surface.

The bonding calculated for LDA, GGA and B3LYP density functional approximations show similar features and the results obtained for the adsorption energies imply relatively weak interactions between adsorbed metal atoms and MgO surface. However, the transition metal atoms on MgO surface calculated within the LD approximation (Figs. 4 and 5) are more polarized and more electron density is transferred from the surface oxygen atoms to the metal orbitals.

The metal atoms experience stronger interaction with the surface and in addition more antibonding $4d_z^2$ states are pushed above the Fermi level. This enhances the covalent part of the bonding and the adsorption energy is larger. For the TM atoms on the MgO surface calculated with the GGA approximation the charge density is more localized on the atoms and less electron density is transferred to the metal. The polarization of the adsorbed metal atoms is thus restrained and yields weaker electrostatic interaction which in turn decreases the covalent part of the metal–oxygen bond (less antibonding filled states are pushed over Fermi level), therefore the adsorption energy is smaller.

4. Conclusion

The adsorption geometry and electronic properties of Pd and Rh atoms deposited on the (2×2) (100)MgO surface were analyzed by means of periodic DFT calculations. The structural optimization was performed using local, gradient-corrected and hybrid B3LYP functionals. The calculations show that the metal atom prefers

on top adsorption, above the surface oxygen in agreement with the trends in the recent FP-LMTO calculations. We found a stable geometry also for the adsorption of the metal in a bridging position above the surface at 2.081 Å for Pd (B3LYP) and 2.106 Å for Rh (B3LYP), respectively.

We have studied details of the electronic structure of Pd and Rh adsorbed on top of the oxygen and bridging two oxygens on the (100) surface of MgO. The bonding between the metal and the oxygen(s) for both optimized structures is partly covalent with contribution from polarization attraction. The trend of the variations of the adsorption energies calculated and PDOS for LDA, GGA and B3LYP approximations suggest that these variations are dominated by electrostatic effects. For the levels of approximation applied in this work we observe small electron transfer of 0.2–0.3 e^- from the support to the metal. The electrostatic effects are stronger for LDA approximation where the electronic transfer is the largest and the contribution of the polarization attraction to the bonding and thus the adsorption energy is the highest.

We find that Rh adsorption on the (100)MgO surface follows the tendency to adsorb above surface oxygens with spin-polarized (doublet) ground state. The spin-polarization effects found to be less pronounced at the LDA and GGA levels were obtained to be significant with the B3LYP functional. The Rh atom binds stronger to the substrate than the Pd probably due to the stronger polarization effects and larger electrostatic attraction.

Acknowledgements

The authors are grateful for partial financial support of NATO linkage grant No PST.CLG.977625, Grant No VUH-1705 of the Bulgarian National Science Foundation and of Università della Calabria.

References

[1] C.R. Henry, Surf. Sci. Rep. 31 (1998) 231.
[2] H.J. Freund, Surf. Sci. 500 (2002) 271.
[3] V.A. Nasluzov, V.V. Rivanenkov, A.B. Gordienko, K.M. Neyman, U. Birkenheuer, N. Roesh, J. Chem. Phys. 115 (2001) 8157.
[4] S. Abbet, E. Riedo, H. Brune, U. Heiz, A.-M. Ferrari, L. Giordano, G. Pacchioni, J. Am. Chem. Soc. 123 (2001) 6172.
[5] L. Giordano, C. Di Valentin, J. Goniakowski, G. Pacchioni, Phys. Rev. Lett. 92 (2004) 096105.
[6] L. Giordano, C. Di Valentin, G. Pacchioni, J. Goniakowski, Chem. Phys. 309 (2005) 41.
[7] A. Del Vitto, L. Giordano, G. Pacchioni, U. Heiz, J. Phys. Chem. B 109 (2005) 3416.
[8] K. Judai, A.S. Wörz, S. Abbet, J.-M. Antonietti, U. Heiz, A. Del Vitto, L. Giordano, G. Pacchioni, Phys. Chem. Chem. Phys. 7 (2005) 955.
[9] A. Del Vitto, G. Pacchioni, F. Delbecq, P. Sautet, J. Phys. Chem. B 109 (2005) 8040.
[10] A.S. Wörz, K. Judai, S. Abbet, J.-M. Antonietti, U. Heiz, A. Del Vitto, L. Giordano, G. Pacchioni, Chem. Phys. Lett. 399 (2004) 266.
[11] J. Goniakowski, Phys. Rev. B 57 (1998) 1935.
[12] J. Goniakowski, Phys. Rev. B 58 (1998) 1189.
[13] J. Goniakowski, Phys. Rev. B 59 (1999) 11047.
[14] L.N. Kantorovich, J.M. Holender, M.J. Gillan, Surf. Sci. 343 (1995) 221.
[15] W. Vervisch, C. Mottet, J. Goniakowski, Phys. Rev. B. 65 (2002) 245411.
[16] J. Goniakowski, C. Noguera, Phys. Rev. B 60 (1999) 16120.
[17] A. Stirling, I. Gunji, A. Endow, Y. Oumi, M. Kubo, A. Miyamoto, J. Chem. Soc. Faraday Trans. 93 (1995) 1175.
[18] R. Wu, A.J. Freeman, Phys. Rev. B 51 (1995) 5408.
[19] S. Nokbin, J. Limtrakul, K. Hermansson, Surf. Sci. 566–568 (2004) 977–982.
[20] A. Bogicevic, D.R. Jenisson, Surf. Sci. 515 (2002) L481.
[21] G. Xi, J. Bao, S. Chao, S. Li, J. Vac. Sci. Technol. A 10 (1992) 2351.
[22] T. Yamada, I. Matsuo, J. Nakamura, M. Xie, H. Hirano, Y. Yamatsumoto, K.I. Tanaka, Surf. Sci. 231 (1990) 304.
[23] X. Xu, P. Chen, X. Xu, D.W.. Goodman, Phys. Chem. 98 (1994) 9242.
[24] X. Xu, D.W. Goodman, Catal. Lett. 24 (1994) 31.
[25] S.M. Vesecky, D.R. Reiner, D.W. Goodman, J. Vac. Sci. Technol. A 13 (1995) 1539.
[26] M. Date, H. Okyama, N. Takagi, M. Nishijima, T. Aruga, Surf. Sci. 350 (1996) 79.
[27] M. Hirsimaki, S. Suhonen, J. Pere, M. Valden, M. Pessa, Surf. Sci. 402 (1998) 187.
[28] I. Kobal, K. Kimura, Y. Ohno, T. Matsushima, Surf. Sci. 445 (2000) 472.
[29] L. Piccolo, C.R. Henry, J. Mol. Catal. A Chem. 167 (2001) 181.
[30] V.R. Saunders, R. Dovesi, C. Roetti, M. Causa, N.M. Harrison, R. Orlando, C.M. Zicovich-Wilson, CRYSTAL 98 User's Manual, Univ. of Torino, Torino, 1999.
[31] R. Dovesi, Solid State Commun. 54 (1985) 183.
[32] P.J. Hay, W.R. Wadt, J. Phys. Chem. 82 (1985) 284.
[33] C. Lee, W. Yang, R.G. Parr, Phys. Rev. B 37 (1988) 785;
A.D. Becke, J. Chem. Phys. 98 (1993) 5648.
[34] P.A.M. Dirac, Proc. Cambridge Philos. Soc. 26 (1930) 376.
[35] J.P. Perdew, A. Zunger, Phys. Rev. B 23 (1981) 5048.
[36] J.P. Perdew, Y. Wang, Phys. Rev. B 33 (1986) 8800.
[37] J.P. Perdew, Y. Wang, Phys. Rev. B 40 (1989) 3399.
[38] R.W.G. Wickoff, Crystal Structure, vol. 1, Interscience Publ., New York, 1965.
[39] M.I. McCarthy, N.M. Harrison, Phys. Rev. B 49 (1994) 8574.
[40] S.H. Suh, V. Alexiev, N. Neshev, G. Munteanu, C. Lepadatu, V. Chihaia, Rev. Roum. Chim. 47 (2002) 663.
[41] P.A. Maksym, Surf. Sci. 149 (1985) 157.
[42] D.L. Blanchard, D.L. Lessor, J.P. LaFemina, D.R. Baer, W.K. Ford, T. Guo, J. Vac. Sci. Technol. A 9 (1991) 1814.
[43] P.W. Tasker, J. Phys. C 12 (1979) 4977.
[44] M.D. Towler, N.M. Harrison, M.I. McCarthy, Phys. Rev. B 52 (1995) 5375.
[45] R.A. Evarestov, A.V. Bandura, Int. J. Quant. Chem. 100 (2004) 452.
[46] U. Schonberger, F. Aryasetiawan, Phys. Rev. B 52 (1995) 8788.
[47] R.J. Emrich, A.N. Mansour, D.E. Sayers, S.T. McMillan, J.R. Katzer, J. Phys. Chem. 91 (1987) 3772.
[48] G. Haas, A. Menck, H. Brune, J.V. Barth, J.A. Venables, K. Kern, Phys. Rev. B 61 (2000) 11105.